ADVANCED BIOSYSTEMS

Supporting Information

for *Adv. Biosys.*, DOI: 10.1002/adbi.201800228

Profiling Heterogeneous Circulating Tumor Cells (CTC) Populations in Pancreatic Cancer Using a Serial Microfluidic CTC Carpet Chip

Mina Zeinali, Vasudha Murlidhar, Shamileh Fouladdel, Shimeng Shao, Lili Zhao, Heather Cameron, Armand Bankhead III, Jiaqi Shi, Kyle C. Cuneo, Vaibhav Sahai, Ebrahim Azizi, Max S. Wicha, Mathias Hafner, Diane M. Simeone, and Sunitha Nagrath**

Supplementary data

Cell culture and cell tracker dye protocol

Four different cancer cell lines, human colon adenocarcinoma cell line (HT-29), human pancreatic cell line (Panc-1), human prostate cancer cell line (PC-3), and human breast cancer cell line (Hs-578T) were obtained from ATCC. Capan-1 cancer cell line was obtained from Dr. Howard Crawford's lab (University of Michigan). The HT-29 cells were cultured in McCoy's 5A Medium (30-2007 ATCC), PC-3 and Hs-578T cells in low-glucose Dulbecco's modified Eagle's- F12 (DMEM-F12) (Invitrogen) medium, Panc-1 cells in DMEM+++ (Invitrogen), and Capan-1 cells in IMDM (HyClone), all supplemented with 10% fetal bovine serum (FBS) (Invitrogen), and 1% penicillin-streptomycin (Sigma).

Cultures were maintained at 37°C in a humidified atmosphere containing 5% (v/v) CO_2. The cells were cultured in sterile 25 or 75 cm^2 flasks (Corning) and media replaced every 48 hr. Sub-confluent monolayers of cells were detached using Trypsin/EDTA solution and washed in standard media, followed by centrifugation at 1000 RPM for 5 min. The cell pellet was washed two times with PBS and resuspended with 5 mL of serum free media plus 5 µL dye (Green CellTracker (GCT) (Invitrogen), followed by incubation for 30 min at 37°C. The cells were washed with PBS and incubated in complete media at 37°C for 30 min. After washing the pellet with PBS, 1000 cells per mL were prepared by serial dilution. Labeled cells were spiked into PBS or healthy control (HC) blood for CTC Carpet Chip testing.

Engineering Design, Microfabrication and Surface functionalization

Microfabrication is the method of fabrication of miniature structures of micro-nanometer scales. The pattern was first designed, fabricated (by photolithography), bonded to a substrate and then finally surface functionalized (Figure S1A).

The design was converted to a photomask (FineLine Imaging) and used for fabrication using traditional soft photolithography [37] (Figure S1B). Photolithography is a process by which an image is optically transferred from one surface to another, most commonly by the projection of light through a mask onto a photosensitive material such as photoresist. Photoresists are radiation sensitive materials that typically consist of a polymer resin, a radiation sensitizer, and a carrier solvent. Photoresist can be classified as either positive or negative based on their solubility following UV exposure. The solubility of exposed areas in positive resists increases, whereas in the negative photoresist the solubility is decreased.[38] Generally, a negative photoresist is strengthened by radiation exposure so the remaining pattern after being subject to a developer solution appears as the inverse of the opaque regions of the mask.

In our study, SU-8 100 (MicroChem Corp) was selected as a negative photoresist, and was used to prepare a mold with a final thickness of range 100 µm. The SU-8 was spin coated onto a silicon wafer at 500 rpm for 10 sec and then 2350 rpm for 60 sec. This was followed by two steps of soft baking, first at 65°C for 10 min and then 95°C for 1 hr, after which the coated wafer was exposed to UV light for 15 sec using a Karl Suss MA6 aligner. Post exposure baking was done first at 65°C for 3 min followed by 95°C for 10 min and the pattern was developed in SU-8 developer for 2 min, followed by rinsing with isopropyl alcohol for 2 min and hard baking at 150°C for 3 min. The resulting thickness was confirmed to be within the range of 98-100 A° as determined using Dektak 6M Surface Profilometer. The steps involved in photolithography techniques for our study were shown in Figure S1B.

For rapid prototyping the microfabrication of the chambers was done using an elastomer 4 polydimethylsiloxane (PDMS) (Dow Corning®), which is not only optically transparent, but also allows for additional histochemical stains and markers to be applied post-enumeration, and

is conducive to bright field imaging (currently a limitation in the silicon CTC Chip). PDMS is a flexible elastomeric polymer that is an excellent material for microfluidic device fabrication. In present studies we have used one of the most common PDMS elastomers, Sylgard® 184 (Dow Corning). Sylgard is a two part resin system containing vinyl groups and hydrosiloxane groups. Mixing the two resin components together leads to a cross-linked network of dimethyl siloxane groups. Because this material is flexible, it can be unmolded (peeled) from the SU-8 master, leaving the master intact and ready to produce another device.

In order to produce an inexpensive, disposable, high throughput point-of-care multiplex microfluidic device, the current design is reproduced in transparent polydimethylsiloxane (PDMS) elastomer. PDMS (mixed in a 10:1 ratio of PDMS base with curing agent, Sylgard® 184) was degassed in a desiccator for about 30 min, after which it was cast over the SU-8 mold, and degassed again for about 2 hr. Degassed PDMS was placed in an oven at 65°C overnight. The cured PDMS casting was released by peeling it away from the mold and fluidic ports were punched was done at the designated ends of the chamber to create inlet and outlet holes. These holes were later used for incorporating tubing inputs. The punched hole was slightly smaller than the outer diameter of the tubing being used. Providing adequate sealing for typical fluidic pressures. The schematic of the rapid prototyping of PDMS devices and its bonding to glass slides is shown in Figure S1C.

One of the most useful properties of PDMS is that its surface can be chemically modified in order to obtain the interfacial properties of interest. The most reliable method to covalently functionalize[37] PDMS is to expose it to oxygen plasma, whereby surface Si-CH_3 groups along the PDMS backbone are transformed into Si-OH groups by the reactive oxygen species in the plasma. These silane surfaces are easily transformed with alkoxysilanes to yield much different

chemistry. PDMS replicas and glass slides were cleaned with oxygen plasma and then immediately placed in contact to bond the surfaces irreversibly. The PDMS slab was bonded with a glass substrate , post oxygen plasma treatment for oxidization the surfaces, and therefore for having a hydrophilic area, along with a 10 min baking at 80°C hot plate for having a stronger bonding Figure S1C.

The chemical modification and functionalization of the surface of the device was done immediately after the bonding as depicted (Figure S1D). Initially, the surface of the device was modified with 4% (v/v) 3-mercaptopropyl trimethoxy silane (Gelest) in ethanol (1:25 ratio) for making the surfaces more hydrophilic, at room temperature for 1 hr. Then it was treated with the coupling agent *N*-gamma-Maleimidobutyryloxy-Succinimide (GMBS) (Pierce) in ethanol (1:357 ratio) for 30 min, resulting in GMBS attachment to the microposts as a linker. Next, the device was treated with 100 µg mL^{-1} Neutravidin (Invitrogen) in phosphate buffered saline (PBS) 1:10 ratio) at room temperature, leading to immobilization onto GMBS, and then flushed with PBS to remove excess of avadin. Finally, biotin-conjugated anti-Epithelial cell adhesion molecule (EpCAM) (RnD Systems) antibodies or anti-CD133 (Miltenyi Biotec) antibodies at a concentration of 20 µg mL^{-1} in PBS with 1% (w/v) Bovine Serum Albumin (BSA) was allowed to react for 30 min for each inlet and outlet before washing with PBS. The device was immediately used for capturing CTCs or cancer cells (Figure S1D).

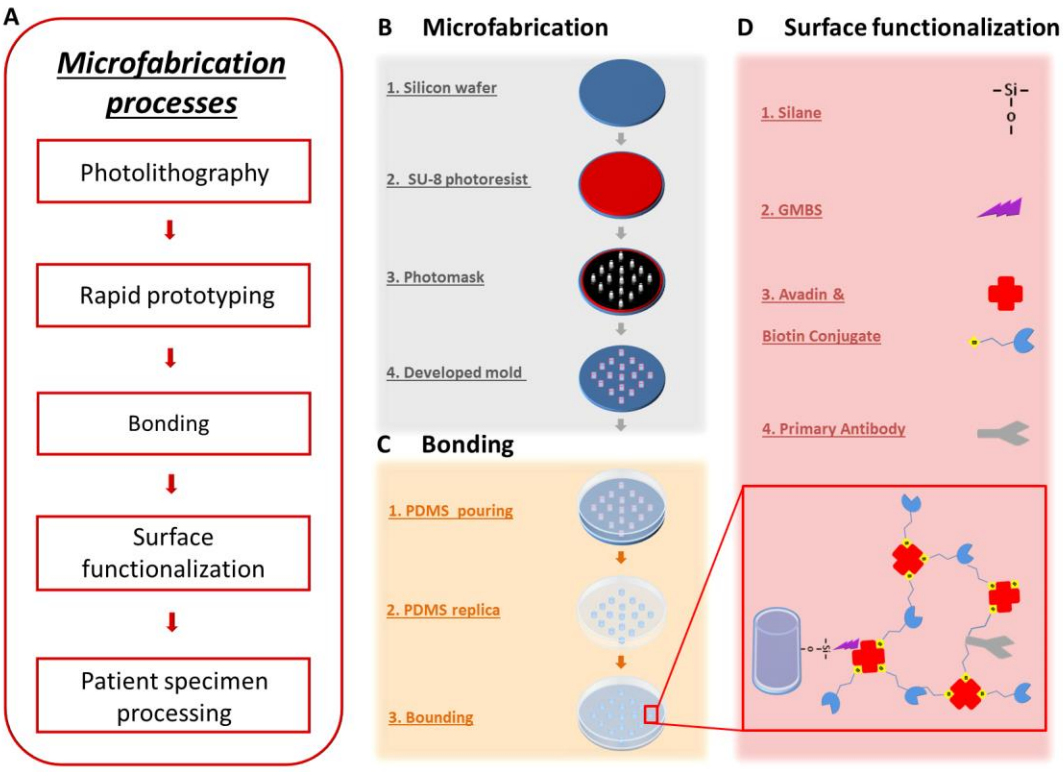

Figure S1: A The flow chart of the microfabrication processes of the microfluidic CTC Carpet Chip, Photolithography, rapid prototyping and bonding and surface functionalization steps. Microfabrication process using traditional soft photolithography (B), Rapid prototyping and bonding (C), and Surface functionalization (D).

Different designs configuration of devices

We undertook a pilot exploratory study comparing four different CTC Chips to determine the highest CTC capture efficiency. Different micropost distributions and arrangement were tested in this study including, the CTC Original, Modified (both had pattern of repetition of 10 × 10 arrays of 100 µm posts), Rotated and Carpet Chip. The Modified device was different versions of the Original CTC Chip with some changes on the outliers to make them more specific and sensitive for capturing purpose (Figure S2A-B).

In the Rotated device, these arrays were rotated 10° relative to the previous array until reaching a total rotation of 180° and then decreasing rotation from 180° to 0° for the subsequent row (Figure S2C). The CTC Carpet Chip is based on an 18° rotation of hexagonal arrays of 100µm posts (Figure S2D). Among all other CTC Chips, CTC Carpet Chip showed the highest

% capture efficiency of spiked GCT PC-3 cell line into buffer/blood at 1 mL hr^{-1} as well as the purity among the other tested CTC Chips (Figure S2E). The summary of the comparison between different devices are mentioned in Table S3.

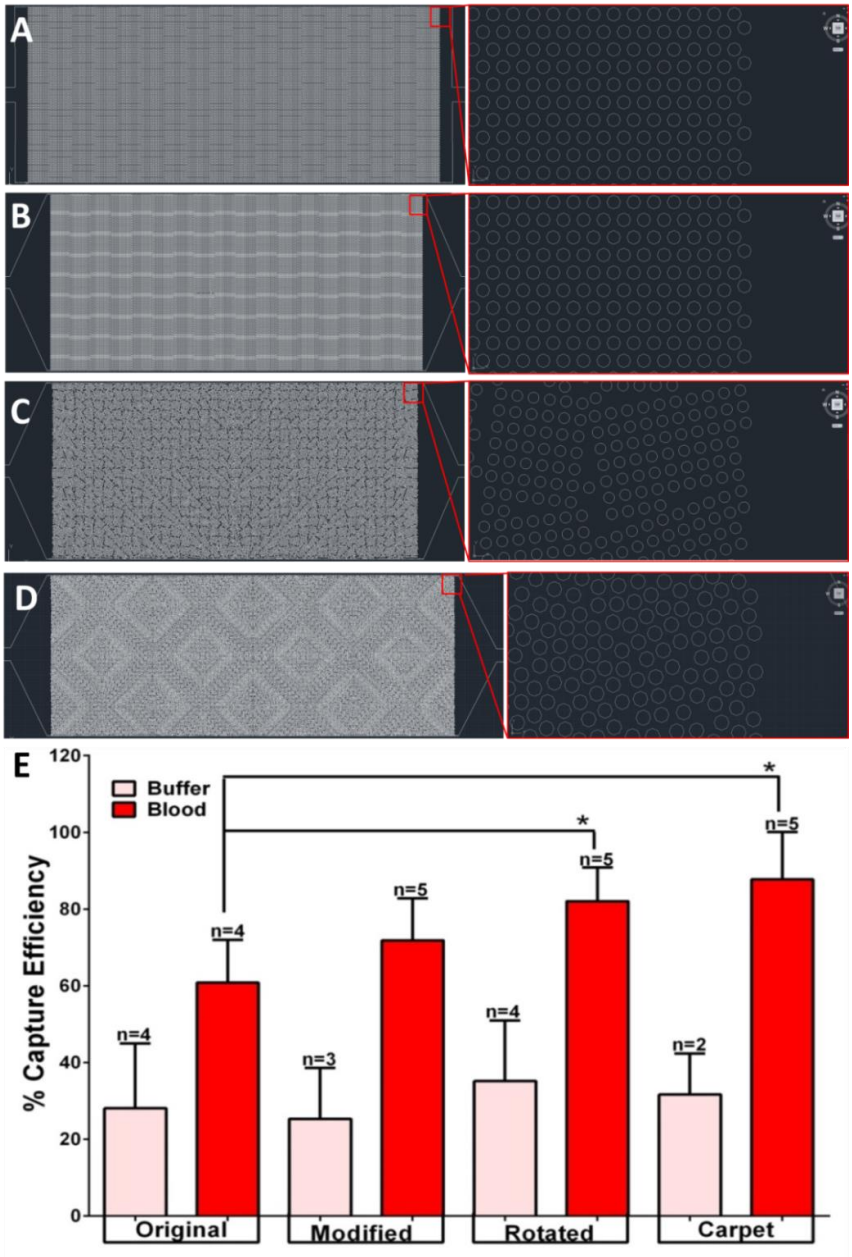

Figure S2: Different configuration of the CTC Chip. **A** Original, **B** Modified, **C** Rotated, **D** Carpet. **E** The comparison between different microfluidic devices. EpCAM capture efficiency (%) with pre-labeled cancer cells (PC-3) spiked into buffer and blood in 4 different CTC Chip, including Original, Modified, Rotated and CTC Carpet Chip. The Carpet CTC Chip showed the highest capture efficiency with PC-3 spiked into blood (87.73%) compared to the other CTC-Chips.

CTC Carpet Chip optimization

Different distance sizes between hexagonal arrays (50 µm and 25 µm) in the CTC Carpet Chip were analyzed. The results indicated that 50 µm distance showed the highest % capture efficiency (94.9%) with the Panc-1 cell line compared to 25 µm distance (Figure S3A). To be able to increase the % purity, the effect of the forward (from inlet to outlet) and backward (from outlet to inlet) PBS wash were also checked within different CTC chips (Original, and Carpet). Backward washing had higher % purity in the CTC Carpet Chip (76.4%) compare to the forward washing (14%) (Figure S3B). The effects of different flow rates on the capture efficiencies were analyzed using the final version of the CTC Carpet Chip. By increasing the flow rate from 1 mL hr^{-1} to 10 mL hr^{-1}, the capture efficiencies significantly decreased (Figure S3C). Therefore, 1 mL hr^{-1} flow rate was selected as a constant flow rate for the rest of the project. In the Carpet design, the posts are arranged in a way to enhance lateral flow in addition to longitudinal flow. In order to further examine this phenomenon, the number of PC-3 cells captured along the length of the device was calculated. It was found that the density of the captured PC-3 cells in the Carpet device was high near the inlet (Figure S3D) similar density observations were made for the contaminating blood cells (Figure S3E).

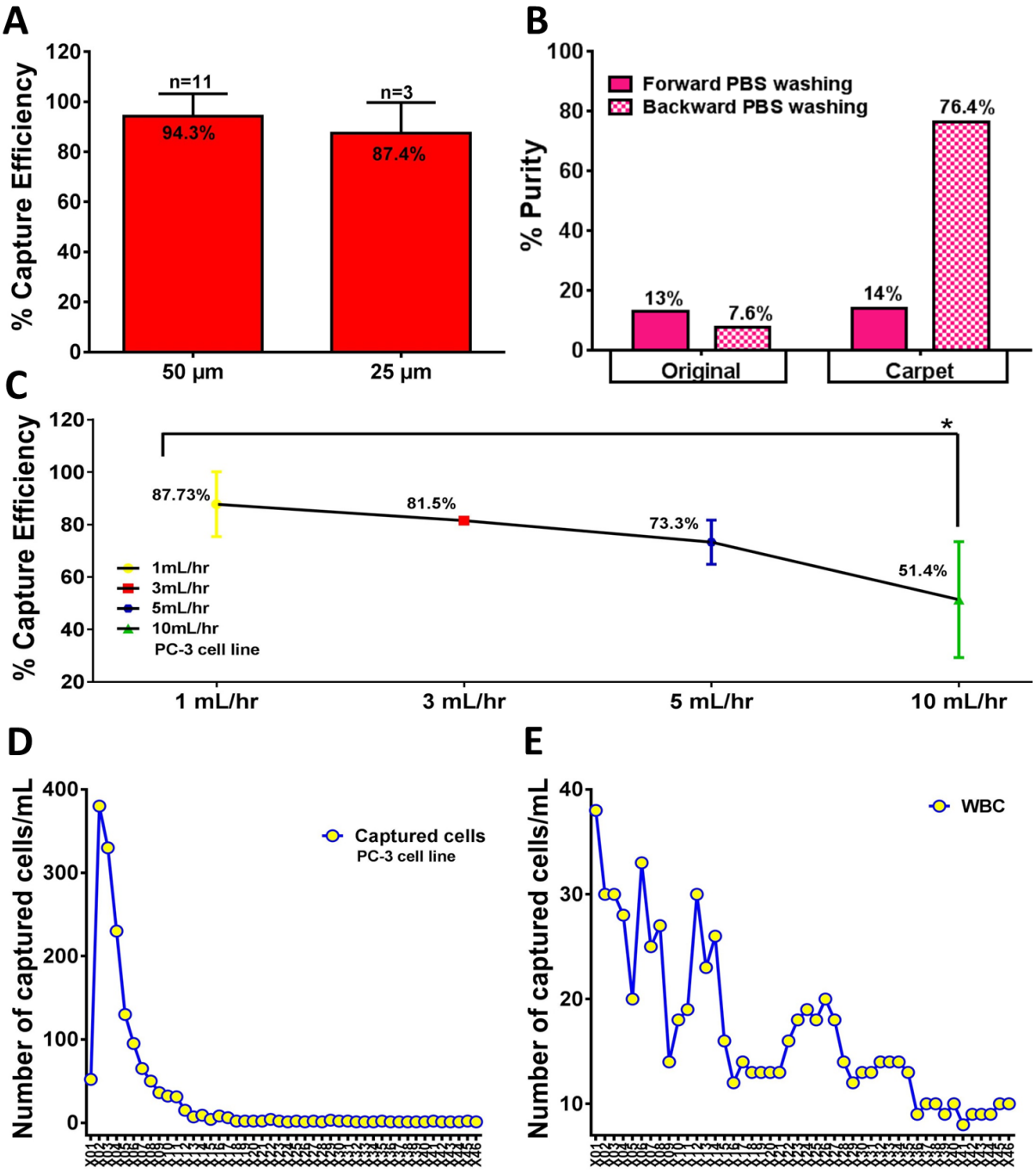

Figure S3: CTC Carpet Chip optimization. **A** Comparison of different distances between hexagonal arrays in the CTC Carpet Chip. The % capture efficiencies were higher in 50 µm distance design. **B** Comparison between backward and forward PBS wash on % purity using HT29 cell line in both the original CTC-Chip and CTC Carpet Chip. The highest % purity was achieved applying backward PBS wash in the CTC Carpet Chip (76%). **C** Analyzing the effect of different flow rates on the % capture efficiencies using PC-3 cell lines. **D-E** Profile capturing across the CTC Carpet Chip using PC-3 cell lines. **D** Number of spiked PC-3 cells into blood captured along the X-axis of Carpet device indicates peak capture area near inlet, along with the number of WBCs captured along the X-axis of Carpet device (**E**).

Chip sequence analysis

The effect of the device order (EpCAM Chip connected to the CD133 device (EpCAM → CD133: Ep1/CD2) and vice versa (CD133 → EpCAM: CD1/Ep2) on capture efficiencies of the spiked GCT Panc-1 cell line into blood and six PaCa patients was tested (Figure S4).

In the Panc-1 cell line, the capture efficiency of the EpCAM Chip was 70.7% when the EpCAM Chip was run as the first Chip (Ep1) and 31.6% when the EpCAM Chip was conducted as the second Chip (Ep2), while, the efficiency of the CD133 Chip was 15.7% and 7.1% when the CD133 Chip being used as the first (CD1) compared to the second (CD2) Chip, respectively (Figure S4A). The effects of the reverse study on the number of CTCs per mL of 6 different PaCa patient samples are shown in Figure S4B. The numbers of captured EpCs/EMTCs per mL were higher in the Ep1/CD2 (22.5/85.3 CTC per mL) group compare to the CD1/Ep2 (73.5/10 CTC per mL). In summary, the cell line results indicated when the EpCAM/CD133 Chip was arranged as a first device (Ep1 and CD1), the capture efficiencies were higher, while the numbers of captured $EpCAM^{+}/CD133^{+}$ were higher in the Ep1/CD2 group compare to the CD1/Ep2 from PaCa patients.

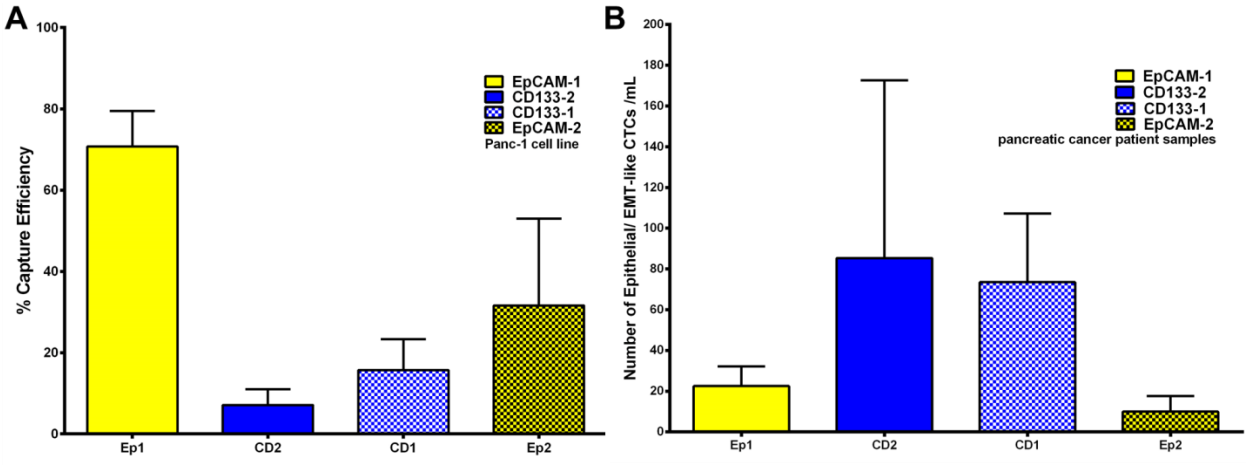

Figure S4: The effect of Chip's order on the numbers of captured cells on dual study. A The effect of reverse study on the capture efficiencies (%) of Panc-1 cell line on different orders of EpCAM vs. CD133 CTC Chips (EpCAM → CD133 (Ep1/CD2) and CD133 → EpCAM (CD1/Ep2)). **B** The effect of reverse study on the number of CTCs per mL

of 6 different PaCa patient samples. Yellow/blue bars show EpCAM/CD133 Chips. Solid bars show EpCAM → CD133 (Ep1/CD2), and hatched bars show CD133 → EpCAM (CD1/Ep2).

Triple staining of Pan-CK, Vimentin and CD45

To determine the presence of EpCs+ in the CD133 Chip and EMTCs+ in the EpCAM Chip, 16 patient samples were tested for triple staining of each Chip (Pan-CK and Vim along with CD45). Two out of 16 samples were Vim+ cells in the EpCAM Chip (1 and 4 cells), and two out of 16 were CK+ cells in the CD133 Chip (2 and 1 cells). As the results show in Figure S5, these markers were relatively specific for their origins, meaning there were few captured EMTCs (mean 0.3 cells per mL) in EpCAM Chips (Figure S5A) and few circulating EpCs in CD133 Chips (median 0.2 cell per mL) (Figure S5B).

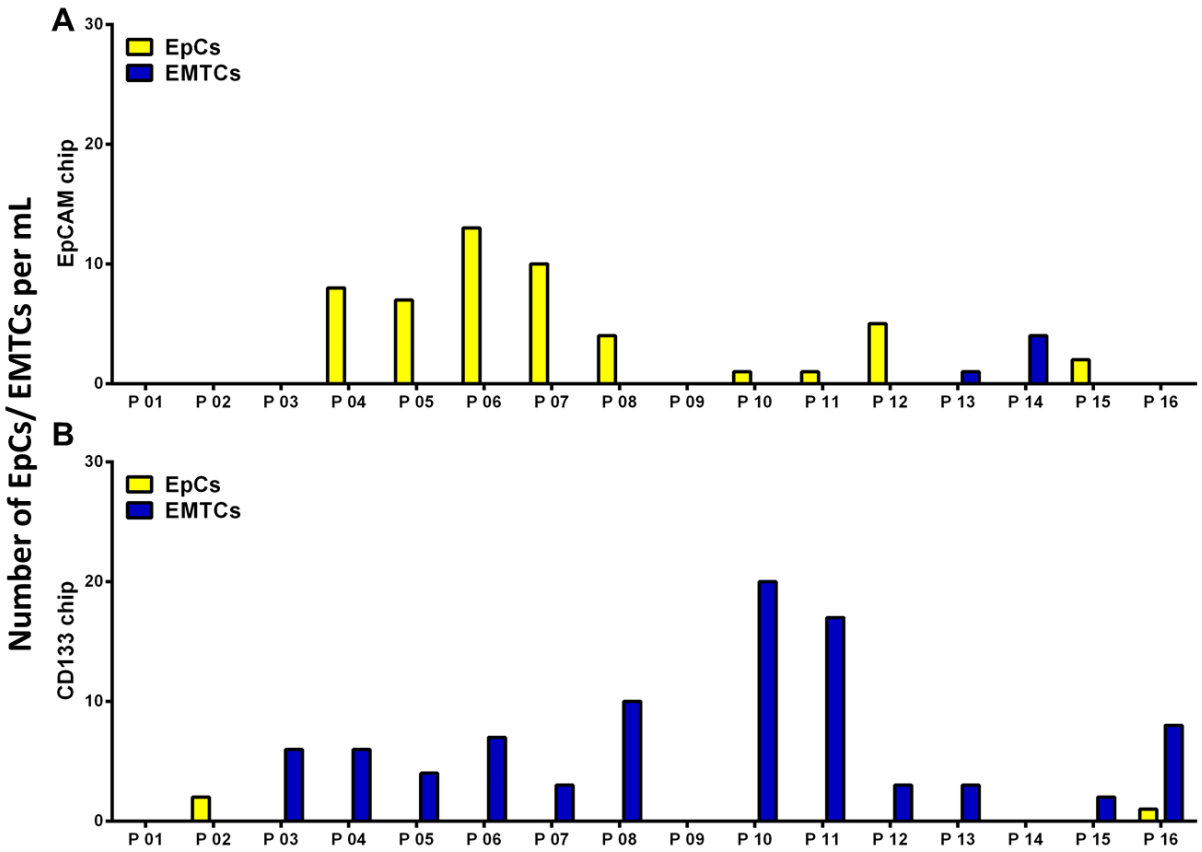

Figure S5: Analysis of 16 PaCa patient samples with triple staining (CK, Vim and CD45) for each CTC Carpet Chip. **A** Analysis of CK and Vim along with CD45 in the EpCAM CTC Carpet Chip. Two out of 16 samples were Vim+ cells in the EpCAM Chip (1 and 4 cells). **B** Analysis of CK and Vim along with CD45 in the CD133 CTC Carpet Chip. A few numbers of samples two out of 16 were CK+ cells in the CD133 Chip (2 and 1 cells).

H&E staining and immunohistochemistry (IHC) analysis of primary tissues

We obtained the PDAC tissues, and stained them for the markers of interest based on analysis of CTCs. We previously showed that genes including CXCR1 and BMi1 have ≥6 log fold change in EpCAM Chip compared to CD133 Chip (Figure 6B). We found that, the primary tissues of early stage patients were highly positive (intensity of 3, 100% positivity) for BMi1 protein expression shown by immunohistochemistry (IHC) analysis (Figure S6A). The H&E staining of the corresponding primary tumor tissue was shown in this figure too.

We also reported that genes including POU5F1 (OCT-4), TP53 and MCAM (CD146) showing ≥5 log fold change in CD133 Chip compared to EpCAM Chip (figure 6B). IHC analysis of TP53 protein expression in the primary PDAC tissue was showed high positivity (intensity of 2, 90% positivity) of this marker (Figure S6B). The H&E staining of the corresponding primary tumor tissue was shown in this figure too. IHC analysis of MCAM protein expression in the primary PDAC tissue was moderate positive (intensity of 2, 30% positivity) (Figure S6C). The H&E staining of the corresponding primary tumor tissue was shown in this figure too. IHC analysis of CD133 protein expression in the primary PDAC tissue was showed different range of positivity (intensity of 1 and 3, 5-60% positivity) of this marker (Figure S6D). The H&E staining of the corresponding primary tumor tissues were shown in this figure too.

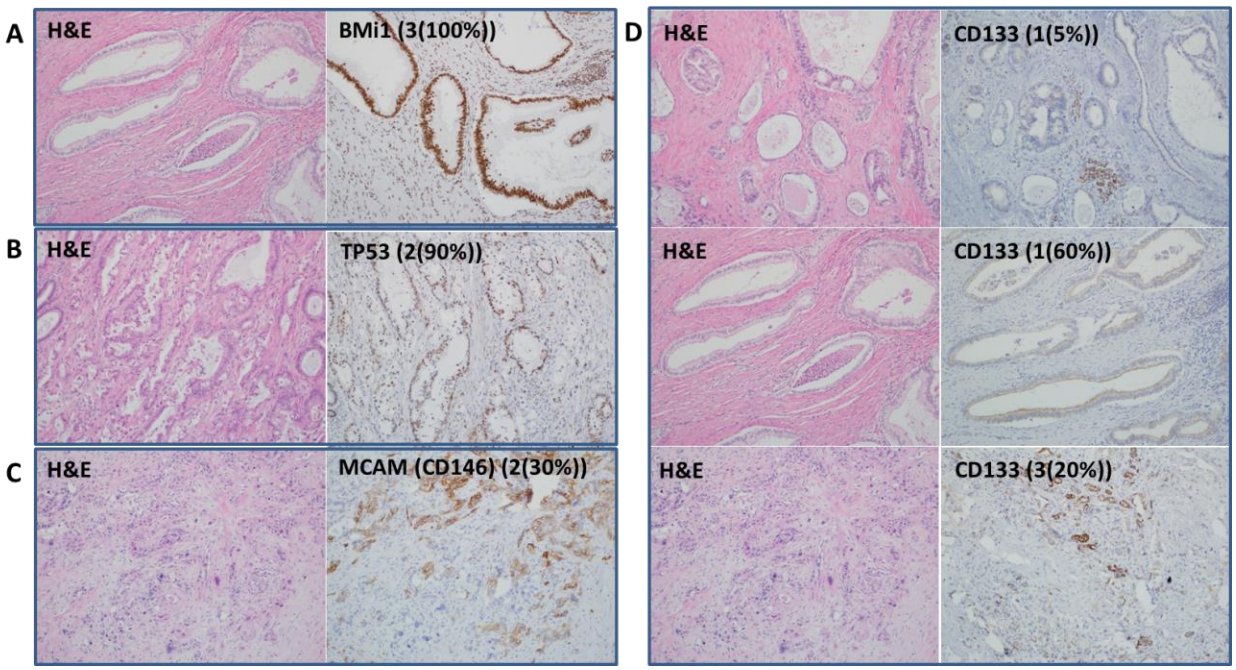

Figure S6: The H&E staining image of the primary tumor tissues of PDAC patients along with immunohistochemistry (IHC) analysis of the corresponding primary tumor tissues A BMi1 protein expressions (intensity of 3 in 100% tumor cells). **B** TP53 marker (intensity of 3 in 90% tumor cells). **C** MCAM marker (intensity of 2 in 30% tumor cells). **D** CD133 marker from different tissue samples (intensity between 1 and 3 in 5-60% tumor cells).

Table S1: Table of 96 genes analyzed by TaqMan Gene Expression Assays

96 genes analyzed by TaqMan Gene Expression Assays											
GAPDH	CD24	KRT5	GLi1	CTNNB1	MAPK	PON1	MMP2	COL1a2	KLF4	MCL1	MKI67
HPRT1	CD44	KRT7	TGFB1	WNT2	CD90	cMYC	MMP9	COL3a1	CXCR1	BAX	PCNA
RAB7A	ALDH1A1	KRT8	Shh	TWIST1	RB1	PDX1	NES	MET	CXCR4	BCL2	CD3D
EPCAM	ALDH1a2	KRT18	TP53	SNAI1	ERCC1	NKX2-1	MGP	BRCA1	IL6	AR	ITGAM
Vimentin	ALDH1a3	KRT19	PTEN	SNAI2	BRAF	IGFBP5	SPON2	CCDC80	IL6R	ESR1	CD14
ERBB2	CD133	KRT20	PIK3CA	ZEB1	ALK	DCN	LGALS3	TIMP1	IL6ST	PGR	MS4A1
EGFR	CCND1	CDH1	AKT1	ZEB2	BMi1	SPARC	ANXA2	TIMP2	IL8	NANOG	CD45
K-Ras	TTF-1	CDH2	ATL1	GEMIN2	ATDC	p63	LGALS3BP	TIMP3	EMP2	POU5F1	MCAM

The 96 cancer-related genes in our study were selected to include epithelial/mesenchymal and stem cell markers, tumor suppressor genes (TSGs), oncogenes, extracellular matrix (ECM), transcription factors and cytokines.

Table S2: Clinical characterization of patients with pancreatic cancer

Patient No.	CTC	EMT	Gender	Age	Stage	T (mm)	N	M	Tumor status	CA19-9 (U/mL)	CEA (ng/mL)	Therapy	Pathology	Death	OS	PFS
P 01	30	26	F	74	IIA	-	N0	M0	Resected	2011	-	Res	AD	Dead	463	279
P 02	25	17	M	51	IIA	-	N0	M0	Resected	44	-	Rad/ Res	AD	Dead	667	494
P 03 ¶*	9	201	M	63	IIA	19	N0	M0	Resected	42	-	Res	AD	Alive	1000	977
P 04 ¶	13	101	M	63	IIA	32	N0	M0	Locally advanced	52	2	No	AD	Alive	907	208
P 05 ¶*	44	73	M	71	IIA	24	N0	M0	Resected	16	-	Res	AD	NA	181	169
P 06	25	44	M	74	IIB	22	N1	M0	Resected	11	-	No	AD	Alive	1508	1292
P 07*	10	77	F	64	IIB	19	N1	M0	Resected	381	-	No	AD	Alive	1314	835
P 08	64	50	M	69	IIB	-	N1	M0	Resected	84	3.3	NA	AD	Alive	1245	1218
P 09 ¶	38	92	M	65	IIB	45	N1	M0	Locally advanced	524	4	No	AD	Dead	612	612
P 10	36	180	M	74	IIB	40	-	M0	Locally advanced	2128	5	No	AD	Dead	223	223
P 11 ¶*	21	118	M	68	IIB	29	N1	M0	Resected	4	7	Res	AD	Dead	319	55
P 12 ¶	16	42	M	76	IIB	18	N1	M0	Locally advanced	688	-	No	AD	Dead	99	99
P 13 ¶	5	127	M	56	IIB	23	N1	M0	Borderline resectable	1033	3	No	AD	Dead	539	471
P 14 *	10	93	M	40	IIB	15	N1	M0	Resected	3	<1	Chemo/Res	AD	Alive	1112	1112
P 15 ¶	9	78	F	55	III	23	N0	M0	Locally advanced	21	2	No	AD	Alive	654	344
P 16	0	15	F	53	III	-	N0	M0	Locally advanced	2485	-	No	AD	Dead	670	573
P 17	8	40	F	60	III	-	N0	M0	Borderline resectable	27	-	Chemo	AD	NA	364	161
P 18	8	26	F	66	III	-	N0	M0	Locally advanced	325	-	NA	AD	Dead	321	321
P 19	9	27	F	70	III	-	N1	M0	Locally advanced	3693	-	No	AD	Dead	602	465
P 20	8	183	F	60	III	13	N1	M0	Locally advanced	619	-	No	AD	Dead	1363	373
P 21 ¶	39	87	F	55	III	17	N0	M0	Locally advanced	21	2	No	AD	Alive	723	351
P 22 ¶	57	73	M	64	III	27	N0	M0	Locally advanced	52	2	No	AD	Alive	1011	1005
P 23 ¶	30	15	M	63	III	44	-	M0	Locally advanced	-	-	No	AD	Dead	482	254
P 24	9	48	F	81	IV	43	-	M1-Liver	Locally advanced	17408	-	Chemo	AD	Dead	519	519
P 25	9	21	M	66	IV	-	N0	M1	Metastatic	1109	-	No	AD	Dead	130	91
P 26	5	105	M	73	IV	-	N1	M1	Metastatic	145	-	NA	AD	NA	14	14
P 27	67	66	F	50	IV	35	-	M1-Liver	Metastatic	-	-	Chemo	AD	Dead	548	72
P 28 ¶	29	147	M	51	IV	34	N1	M1-Liver	Metastatic	4	-	No	AD	Dead	131	52
P 29	31	36	F	58	IV	39	N1	M1-Breast	Metastatic	56	29	No	AD	Dead	167	99
P 30 ¶	13	51	M	60	IV	44	N0	M1-Lung	Metastatic	4232	-	No	AD	Dead	367	137
P 31 ¶	35	236	M	66	IV	80	N1	M1-Liver	Metastatic	3116	12	No	AD	Dead	450	55

P 32 ¶	13	128	M	74	IV	56	N1	M1-Peritoneum	Metastatic	45	9	No	AD	Dead	169	139
P 33 ¶	9	83	M	65	IV	65	N1	M1-Liver	Metastatic	652518	-	No	AD	Dead	437	169
P 34 ¶*	44	207	M	78	IV	60	N1	M1-small bowel	Metastatic	19712	26	No	AD	Dead	76	76
P 35	7	85	F	58	IV	60	N1	M1-Liver, Peritoneum	Metastatic	-	-	Chemo/Rad	AD	Dead	734	143
P 36*	-	-	M	64	III	14	N1	M0	Locally advanced	204	1	Chemo	AD	Alive	1127	936
P 37 *	-	-	F	65	IIB	29	N1	M1-Liver	Metastatic	97	-	Chemo/Rad	AD	Alive	496	265
P 38 *	-	-	F	78	IIB	15	N1	M1-Liver	Metastatic	132	-	Chemo	Ad	Alive	440	440
P 39 *	-	-	F	74	IIA	30	N0	M1-Liver	Metastatic	29	<1	Chemo	AD	Dead	462	134
P 40 *	-	-	M	61	IIA	22	N0	M1-Liver	Metastatic	21	<1	Chemo	AD	Dead	514	259
HC 01	F	33	0	-	-	-	-	-	-	-	-	-	HC	Alive		
HC 02	F	27	2	-	-	-	-	-	-	-	-	-	HC	Alive		
HC 03	M	27	3	-	-	-	-	-	-	-	-	-	HC	Alive		
HC 04	M	24	1	-	-	-	-	-	-	-	-	-	HC	Alive		
HC 05	F	45	2	-	-	-	-	-	-	-	-	-	HC	Alive		
HC 06	M	40	0	-	-	-	-	-	-	-	-	-	HC	Alive		
HC 07	F	57	6	-	-	-	-	-	-	-	-	-	HC	Alive		
HC 08	M	90	3	-	-	-	-	-	-	-	-	-	HC	Alive		
HC 09	M	66	0	-	-	-	-	-	-	-	-	-	HC	Alive		

CA19-9, Carbohydrateantigen19-9; CEA, carcinoembryonic antigen; Chemo, Chemotherapy; Rad, Radiation; Res, Resected; AD, Adenocarcinoma; NA, not Available; HC, healthy controls; OS, overall survival; PFS, progression free survival. RNA analyses were done for patients marked with ¶. Tissues samples of patients marked with* were analyzed for IHC analysis.

Table S3: Comparison of several microfluidic devices:

Microfluidic Devices	Array	Rotation
Original	10 × 10	-
Modified	10 × 10	-
Rotated	10 × 10	10°
Carpet	8 × 8	18°